ORGANIC LETTERS

2001
Vol. 3, No. 3
357−360

Connectivity Effects in Isomeric Naphthalenedinitrenes

Paul R. Serwinski,[†] Richard Walton,[†,1] Jon A. Sanborn,[†,2] Paul M. Lahti,*[,†] Tomonori Enyo,[‡] Daisuke Miura,[‡] Hideo Tomioka,*[,‡] and Athanassios Nicolaides[§]

Department of Chemistry, University of Massachusetts, Amherst, Massachusetts 01003, Department of Materials Science, Mie University, Tsu, Mie, 5148507 Japan, and Department of Chemistry, University of Cyprus, Nicosia 1678, Cyprus

lahti@chem.umass.edu

Received November 6, 2000

ABSTRACT

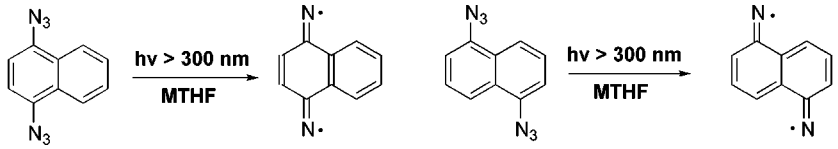

UV–vis, FTIR, and ESR spectroscopic studies were carried out on samples of 1,4- and 1,5-naphthalenediazide that were photolyzed at cryogenic temperatures in argon and frozen solvent matrices. Mononitrenes and diiminediyl systems are produced. Spectral and computational results are consistent with quinonoidal singlet ground-state structures for the diiminediyls, rather than aromatic dinitrene structures.

One interesting question in organic electronic structure theory involves the interplay between electron pairing to form bonds in a conjugated system versus the tendency of polycyclic aromatic π-networks to form aromatic rings. Electron pairing tends to overcome aromatization, so the Kekulé xylylenes are reactive olefins with biradicaloid character. However, the biradical nature of 2,2-dimethyl-*2H*-dibenzo[*cd*,*k*]fluoranthene[3] shows that aromatization *can* overwhelm Kekulé-type valence bond electron pairing, when conjugative bonding has an insufficient driving force.

Various species have been derived by the generation of two nitrene or carbene sites with direct conjugation (Scheme 1). All of **1**−**3** (Scheme 1) have quinonoidal structures, based upon UV, FTIR, and ESR spectral analysis plus computational studies.[4−10] Systems of general type **4** with various linkers -X- likewise have quinonoidal, not aromatic dinitrene structures.[8a,11,12] In these and related systems, the maximum double bond count tends to be achieved, leaving two relatively isolated electrons that exchange couple through spin polarization[11] of the π-electrons in the conjugated network.

Scheme 1

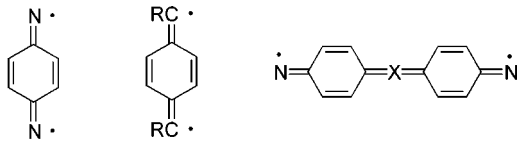

1 **2** R=Ph **3** R=H **4** (X = [direct bond], $[=CH-CH=]_n$, =N-N=)

Dinitrenes with a less direct connectivity path for formation of quinonoidal systems have not been much studied.

[†] University of Massachusetts.
[‡] Mie University.
[§] University of Cyprus.

(1) Present address: Ethox Chemicals, Greenville, SC 29605, USA.
(2) Present address: Amherst College, Amherst, MA 01002, USA.

(3) McMasters, D. R.; Wirz, J.; Snyder, G. J. *J. Am. Chem. Soc.* **1997**, *119*, 8568.
(4) Reiser, A.; Wagner, H. M.; Marley, R.; Bowes, G. *Trans. Faraday Soc.* **1967**, *63*, 2403.
(5) Nicolaides, A.; Tomioka, H.; Murata, S. *J. Am. Chem. Soc.* **1998**, *120*, 11530.
(6) Trozzolo, A. M.; Murray, R. W.; Smolinsky, G.; Yager, W. A.; Wasserman, E. *J. Am. Chem. Soc.* **1963**, *85*, 2526.
(7) Singh, B.; Brinen, J. S. *J. Am. Chem. Soc.* **1971**, *93*, 540.
(8) (a) Minato, M.; Lahti, P. M. *J. Phys. Org. Chem.* **1993**, *6*, 483−487. (b) Minato, M.; Lahti, P. M. *J. Am. Chem. Soc.* **1993**, *115*, 4532−4539. (c) Ichimura, A. S.; Sato, K.; Kinoshita, T.; Takui, T.; Itoh, K.; Lahti, P. M. *Mol. Cryst. Liq. Cryst. Sci. Technol., Sect. A* **1995**, *272*, 279−88.

10.1021/ol0068288 CCC: $20.00
Published on Web 01/10/2001

To compare the electronic natures of 1,4- versus 1,5-naphthalenediyl conjugation linkers, we studied 1,4- and 1,5-naphthalenedinitrene, **5** and **6**, respectively. In this article, we report[13] generation of these reactive intermediates in cryogenic matrix and describe their UV−vis, FTIR, and ESR spectroscopy.

Systems **5** and **6** were generated by photolysis of the corresponding diazide precursors **7** and **8**, which were in turn synthesized by diazotization/azidification of commercially available naphthalenediamines. Synthetic details and characterization are given in the Supporting Information. Both diazide precursors must be protected from stray light to avoid discoloration. Diazide **8** was particularly photolabile and was sublimed just before use.

UV−vis and FTIR experiments were carried out by subliming samples of **7** or **8** with an argon flow onto the precooled optical window of an Iwatani Cryo Mini closed-cycle cryogenic helium cryostat. UV−vis spectra were obtained with a similar apparatus using frozen 2-methyltetrahydrofuran (MTHF) solutions of precursor azide at <70 K in a copper sample holder with quartz windows. ESR experiments were carried out on diazide samples dissolved in MTHF and subjected to 3-fold freeze−pump−thaw degassing in quartz tubes.

Figures 1 and 2 show the UV−vis spectra obtained in argon matrices at 13 K from photolyses of **7** and **8**. Arrows show the growth of new peaks and decrease of precursor peaks. New UV−vis bands at 243 and 254 nm are seen in Figure 1 from photolysis of **7**. These are analogous to bands assigned to **1** in earlier work[4] and are consistent with quinonoidal structure **5**. Figure 2 shows UV−vis bands at 442 and 471 nm attributable to **6** upon irradiation of **8** at 350 nm. Similar peaks are produced in samples photolyzed at <70 K in MTHF matrix. The new UV−vis bands in Figure 2 are reasonable for the conjugated π-network in 1,5-diiminediyl **6**. ZINDO−CIS computations for singlet **6** predict significant UV−vis bands at only at 455 and 465 nm, in good agreement with experiment.[14] Upon extended subsequent photolysis at 254 nm, the UV−vis spectrum

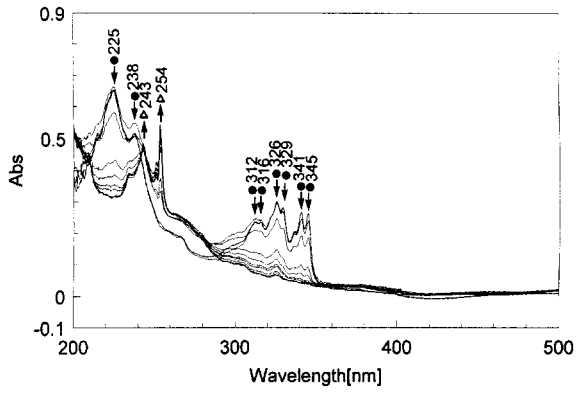

Figure 1. UV−vis spectra from photolysis of Ar matrix isolated **7** at 13 K, >350 nm at intervals. Arrows show peaks that decrease and increase during irradiation. **7** = ●, **5** = △.

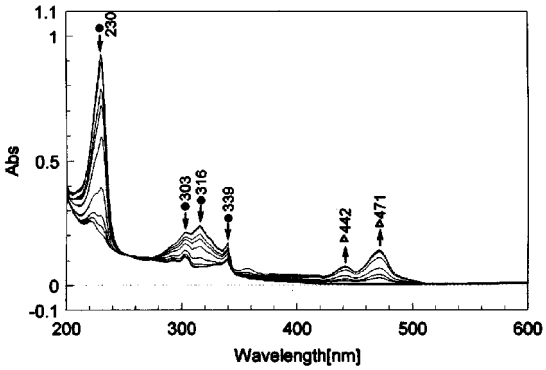

Figure 2. UV−vis spectra from photolysis of Ar matrix isolated **8** at 13 K, >350 nm at intervals. Arrows show peaks that decrease and increase during irradiation. **8** = ●, **6** = △.

assigned to **6** decreases (Supporting Information), concomitant with the growth of a new set of peaks at 329, 340, and 357 nm. On the basis of FTIR spectral data described below, we attribute the new UV−vis peaks to ring-opened species **9**.

Figure 3 shows the results of photolysis of 1,4-isomer **7**. New FTIR bands are observed at 1593, 1481, 1264, 1248, 1155, 998, 811, 761 (s), and 534 cm^{-1}. These bands are similar to those previously observed for the analogous diiminediyl **1**. Figure 4 shows the results of photolysis of 1,5-isomer **8** at 350 nm, which gives new bands at 1279 (w), 1212 (w), 1163 (w), 1033 (w), 758 (m), 749 (s), and 508 cm^{-1} (m). To help with assignment of the vibrational spectra, we carried out hybrid density functional theory (DFT) UB3LYP/6-31G*[15] computations using Gaussian 98[16] and spin-unrestricted GUESS=MIX wave functions for singlet states. This method gives[5] good prediction of the vibrational spectrum for diiminediyl **1**.

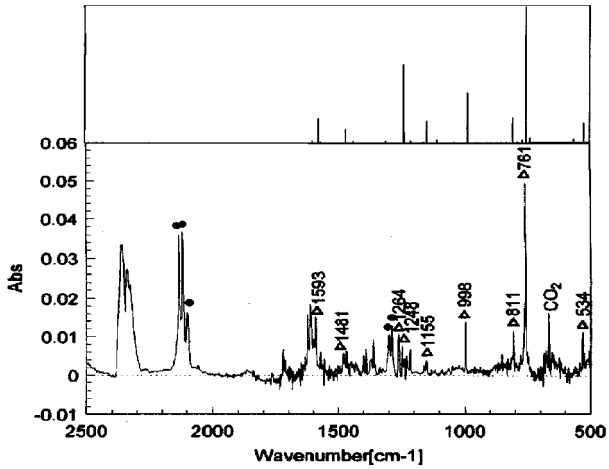

Figure 3. FTIR spectrum from 8-min photolysis of **7** (Ar, 13 K, >350 nm). **7** = ●, **5** = △. Bar graph represents UB3LYP/6-31G* vibrational band positions and relative intensities computed for singlet state **5**.

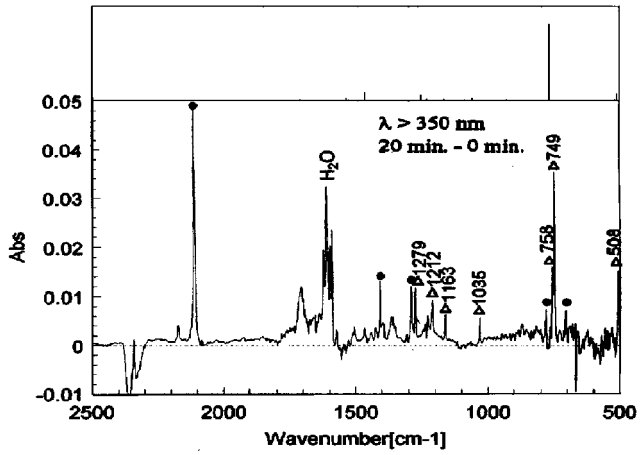

Figure 4. FTIR difference spectrum from 20-min photolysis of **8** (Ar, 13 K, >350 nm). **8** = ●, **6** = △. Bar graph represents UB3LYP/6-31G* vibrational band positions and relative intensities computed for singlet state **6**.

The predicted spectra for both singlet and triplet states of **5** are very good matches for the new bands formed in Figure 3. The singlet state has a spin expectation value of 1.00, showing strong admixture of the triplet state. The biradical singlet and triplet states of **5** are structurally quite similar and give similar computed vibrational bands. The dominance of a band at about 760 cm^{-1} is notable in both predicted and experimental spectra. The quintet dinitrene state, which lies far higher in energy, does not give a good vibrational spectral match, and was not further considered.

The DFT predicted spectrum for the triplet biradical state of **6** includes a dominant 1849 cm^{-1} absorption that is not experimentally observed in Figure 4. By comparison the DFT computed vibrational bands and intensities for the singlet state compare well to the experimentally observed bands, especially the dominance of the experimental band at 749 cm^{-1}. However, the sizable spin contamination of singlet state **6** (spin squared expectation value of 1.78 versus 0.00 theoretical) shows that it is highly admixed with *both* triplet and quintet state character. This renders assignment of the bands in Figure 4 somewhat problematic, but the similarity of photolysate FTIR bands in Figures 3 and 4 suggests structural kinship of the intermediates formed in these experiments.

Finally, we observed that the experimental FTIR spectrum initially formed in Figure 4 is bleached by subsequent photolysis at 254 nm, and a completely new set of peaks is formed (Supporting Information). A new peak at 2225 cm^{-1} is attributable to photocleavage of **6** to give a nitrile such as **9** (Scheme 2), similar to a photofragmentation observed by one[5] of us for **1**.

Scheme 2

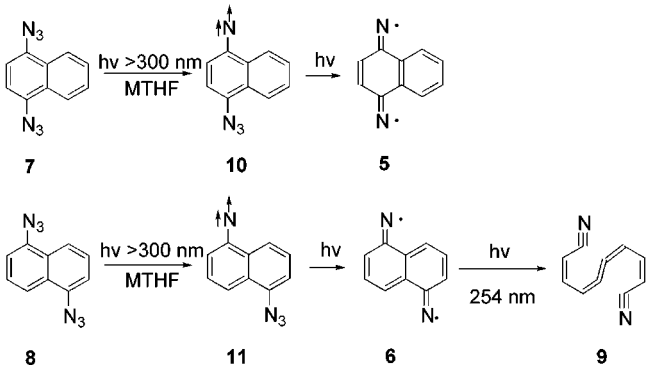

Figure 5 shows the ESR spectrum from photolysis of **7** at 77 K in 2-methyltetrahydrofuran (MTHF). The spectrum shows a mononitrene peak at 6105 G corresponding to a zero field splitting (zfs) of $|D/hc| = 0.74$ cm^{-1}, and a set of peaks at 1497, 2034, 2522(max), 2657, 3835, 3969, 4611 G consistent with triplet biradical **5** having zfs parameters of $|D/hc| = 0.122$ cm^{-1}, $|E/hc| = 0.003$ cm^{-1}. Some low intensity peaks near the typically observed g~2 radical peak suggest a small amount of biradical dimerization analogous that observed by Singh and Brinen[7] in the photolysis of **1**. We attribute the mononitrene peak to product **10** from incomplete azide photolysis in **7**, and the biradical spectrum to diiminediyl system **5** (Scheme 2).

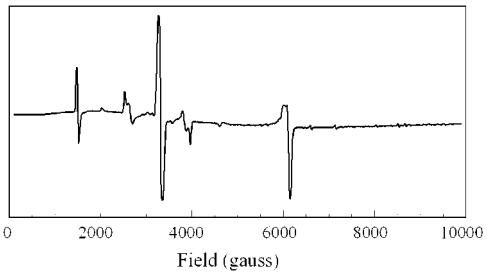

Figure 5. ESR spectrum ($\nu_0 = 9.28$ GHz) from photolysis of MTHF matrix isolated **7** at 77 K, >300 nm (Pyrex) for 5 min.

(9) Yamaguchi, Y.; Sato, K.; Teki, Y.; Kinoshita, T.; Takui, T.; Itoh, K. *Mol.. Cryst. Liq. Cryst. Sci. Technol., Sect. A* **1995**, *271*, 67−78.
(10) Subhan, W.; Rempala, P.; Sheridan, R. S. *J. Am. Chem. Soc.* **1998**, *120*, 11528.
(11) Minato, M.; Lahti, P. M. *J. Am. Chem. Soc.* **1997**, *119*, 2187.
(12) (a) Ohana, T.; Kaise, M.; Yabe, A. *Chem. Lett.* **1992**, 1397. (b) Ohana, T.; Kaise, M.; Nimura, S.; Kikuchi, O.; Yabe, A. *Chem. Lett.* **1993**, 765. (c) Nimura, S.; Kikuchi, O.; Ohana, T.; Yabe, A.; Kaise, M. *Chem. Lett.* **1996**, 125. (d) Nimura, S.; Kikuchi, O.; Ohana, T.; Yabe, A.; Kondo, S.; Kaise, M. *J. Phys. Chem. A* **1997**, *101*, 2083.
(13) Similar results in the UV, FTIR, and ESR spectroscopy from photolysis of **8** have been observed by Tadatake Sato, T.; Niino, H.; Arulmozhiraja, S.; Kaise, M.; Yabe, A., submitted for publication.
(14) ZINDO/S-CIS computations carried out using Hyperchem Pro. 5.1, Hypercube, Inc. See Supporting Information for details.
(15) (a) Becke, A. D. *Phys. Rev. A* **1988**, *38*, 3098−3100. (b) Lee, C.; Yang, W.; Parr, R. G. *Phys. Rev. B* **1988**, *37*, 785.
(16) Frisch, M. J.; Trucks, G. W.; Schlegel, H. B.; Gill, P. M. W.; Johnson, B. G.; Robb, M. A.; Cheeseman, J. R.; Keith, T.; Petersson, G. A.; Montgomery, J. A.; Raghavachari, K.; Al-Laham, M. A.; Zakrzewski, V. G.; Ortiz, J. V.; Foresman, J. B.; Cioslowski, J.; Stefanov, B. B.; Nanayakkara, A.; Challacombe, M.; Peng, C. Y.; Ayala, P. Y.; Chen, W.; Wong, M. W.; Andres, J. L.; Replogle, E. S.; Gomperts, R.; Martin, R. L.; Fox, D. J.; Binkley, J. S.; Defrees, D. J.; Baker, J.; Stewart, J. P.; Head-Gordon, M.; Gonzalez, C.; Pople, J. A. *Gaussian 98*, Rev A.3; Gaussian Inc.: Pittsburgh, PA, 1998.

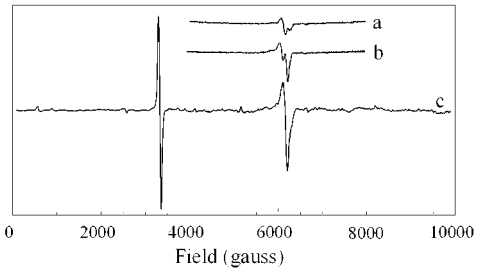

Figure 6. ESR spectrum (ν_0 = 9.33 GHz) from photolysis of MTHF matrix isolated **8** at 77 K: (a) at 350 nm (Oriel band-pass 51830) for 2 min, (b) 350 nm band-pass for another 5 min, (c) then >300 nm (Pyrex) for another 5 min.

UB3LYP/6-31G* and CASSCF/6-31G* singlet−triplet gaps for biradical **5** are computed to be 1.2−4.6 kJ/mol, respectively, favoring the singlet as is typical of diiminediyls.[11−12,17] The aromatic quintet dinitrene **5** lies far above (165−203 kJ/mol) the biradical states and was not further considered. The computations are consistent with observation of a thermally populated triplet biradical ESR spectrum. The computed geometries of the biradical states show bond alternation consistent with a quinonoidal nature.

The ESR spectrum of **5** is similar to that of **1**, consistent with minor structural difference between the two. The zfs in **1** is[11] 0.169 cm^{-1} versus 0.122 cm^{-1} in **5**, showing the effect on the biradical electronic distribution of benzannelation. 4-Azido-phenylnitrene has a zfs of $|D/hc| = 0.90$ cm^{-1},[5−7] while **10** has zfs of 0.74 cm^{-1}. Both **5** and mononitrene **10** should have increased delocalization of π-spin density away from their nitrene nitrogens. With a smaller π-spin on the nitrene nitrogen, the on-center dipolar interactions that dominate the zfs in these systems are reduced,[8a,11] leading to the observed decrease in zfs.

Figure 6 shows the ESR spectrum after 5 min of Pyrex-filtered photolysis of **8** in MTHF at 77 K. It also shows a typical radical byproduct peak, plus a mononitrene peak at 6150 G corresponding to zfs of $|D/hc| = 0.75$ cm^{-1}. As curves a and b show in Figure 6, initial photolysis of **8** yields two mononitrene peaks that gradually merge into one as photolysis continues. Harder and co-workers have shown that photolysis of 4,4′-stilbenediazide undergoes secondary matrix chemistry that results in formation of 4-amino-4′-nitrenostilbene.[18] An analogous process would be a reasonable source of the second mononitrene peak from **8** that arises in addition to the expected mononitrene peak from **11**.

Multiple attempts at photolysis of **8** failed to yield an ESR spectrum corresponding to a biradical triplet state. If such a biradical is present, it must have a singlet ground state with a sufficiently large singlet to triplet energy gap (ΔE(S−T) > 5 kJ/mol) that the triplet biradical is not thermally populated at 77 K. ΔE(S−T) of 1,5-isomer **6** is computed to be a surprising and probably artifactual 20 kJ/mol at the UB3LYP level, due at least in part to the spin contamination problem described earlier. Quintet dinitrene **6** is low in energy relative to the biradical states, only about 14 kJ/mol above the triplet state. The lesser stabilization of quinone-type bond formation in this 1,5-connectivity by comparison to the 1,4-connectivity arises because no aromatic ring-containing resonance structures are retained in the biradical states of **6**.

Because of our concerns about spin contamination in the UB3LYP singlet computations for **6**, we also carried out multiconfiguration SCF computations. CASSCF(6,6)/6-31G* computations[17] yield ΔE(S−T) = 1.0 kJ/mol, while a more robust CASSCF(14,14) subspace gives ΔE(S−T) = 3.7 kJ/mol. CASPT2/6-31G* computations[19] give ΔE(S−T) = 7.9 kJ/mol. These S−T gaps are in better accord than the DFT results with what one expects[5,11−12,20] for diiminediyl biradical states, providing further evidence of the problematic behavior of the singlet versus triplet UB3LYP-DFT results for **6**. The CASSCF and CASPT2 computed S−T gaps remain large enough to be consistent with our failure to observe a triplet biradical ESR spectrum for **6**. CASSCF singlet to quintet energy gaps at these levels are 50−60 kJ/mol, still relatively small by comparison to system **1**.[17] CASPT2 level computations lower the quintet state to 23.5 kJ/mol higher than the biradical states, but overall the quintet remains energetically well beyond thermal excitation at DFT and post Hartree−Fock levels.

In summary, photolysis of 1,4- and 1,5-naphthalenediazides leads to deazetation. The computational and experimental spectroscopic results are consistent with the formation of the corresponding diiminediyl biradicals **5** and **6**. Computations show that the biradical to dinitrene energy spacing is much larger in **5** than in **6**, supporting the notion that quinonoidal bond formation by the indirect path in **6** is less favorable than direct quinone formation across a single phenylene ring.

Acknowledgment. This work was supported by the National Science Foundation (CHE 9809548) and by a Grant-in-Aid for Scientific Research on Specially Promoted Research (12002007) from the Ministry of Education, Culture, Science and Sports in Japan. We thank Dr. Akira Yabe for sharing results[13] of studies of **8** in advance of publication.

Supporting Information Available: Synthetic procedures, ESR spectral simulation **5**, composite figures for experimental and computed FTIR spectral bands and intensities, computational geometries and energies for states of **5** and **6**. This material is available free of charge over the Internet at http://pubs.acs.org.

OL0068288

(17) CASSCF(6,6) computations were carried out using program GAMESS: Schmidt, M. M.; Baldridge, K. K.; Boatz, J. A.; Jensen, J. H.; Koseki, S.; Gordon, M. S.; Nguyen, K. A.; Windus, T. L.; Elbert, S. T. *QCPE Bull.* **1990**, *10*, 52.

(18) Harder, T.; Bendig, J.; Scholz, G.; Stösser, R. *J. Am. Chem. Soc.* **1986**, *118*, 2497−2498.

(19) Some CASSCF and all CASPT2 computations were carried out using the program *MOLCAS* (version 4); Lindh, R.; Malmqvist, P.-Å., Neogrády, P.; Olsen, J.; Roos, B. O.; Sadlej, A. J.; Schutz, M.; Serrano-Andrés, L.; Siegbahn, P. E. M.; Widmark, P.-O. Lund University, Sweden, 1997.

(20) Sanborn, J. A.; Ichimura, A. S.; Lahti, P. M. *J. Phys. Chem. A*, in press.